SAND2005-7790C

Experimental study of scalar filtered mass density function in turbulent partially premixed flames

Danhong Wang and Chenning Tong
Department of Mechanical Engineering
Clemson University, Clemson, SC 29634-0921

R. S. Barlow
Combustion Research Facility
Sandia National Laboratories
Livermore, CA 94551-0969

A. N. Karpetis
Department of Aerospace Engineering
Texas A&M Univesity
College Station, TX 77843

Corresponding author:
Chenning Tong
Department of Mechanical Engineering
Clemson University
Clemson, SC 29634-0921
E-mail: ctong@ces.clemson.edu
Fax: 864 6564435

Colloquium choice: Turbulent flames

Keywords: Turbulent flames, large-eddy simulation, filtered density function, turbulent mixing

Word count (M2):
Text = 4610 words
Figures and Tables = 1175 words
Total = 5785 words

Abstract

The mixture fraction filtered mass density function (FMDF) used in large eddy simulation (LES) of turbulent combustion is studied experimentally. Line images obtained in turbulent partially premixed methane flames (Sandia flames D and E) are used. Cross-stream filtering is employed to obtain the FMDF and other filtered variables. The means of the FMDF conditional on the subgrid-scale (SGS) scalar variance at a given location are found to vary from close to Gaussian to bimodal, corresponding to the well-mixed and nonpremixed SGS mixing regimes, respectively. The bimodal SGS scalar has a structure (ramp-cliff) similar to the counter-flow model for laminar flamelets. Therefore, while the burden on mixing models to predict the well-mixed SGS scalar is expected to decrease with the filter scale, the burden to predict the bimodal one is not. These SGS scalar structures can result in fluctuations of the SGS flame structure between distributed reaction zones and laminar flamelets, but for reasons different from the scalar dissipation rate fluctuations associated with the turbulence cascade. Furthermore, the bimodal SGS scalar contributes a significant amount of the scalar dissipation in the reaction zones, highlighting its importance and the need for mixing models to predict the bimodal FMDFs.

1. Introduction

In LES of turbulent combustion the subgrid-scale (SGS) scalar mixing and the resulting instantaneous (density-weighted) distribution of scalar values in each grid volume, the filtered mass density function (FMDF), must be faithfully represented in order to predict accurately the chemical reaction rate[1, 2, 3]. An important modeling approach uses the FMDF transport equation, in which the reaction source term is in closed form, while the mixing of SGS scalars requires modeling. As a step toward understanding the mixing of multiple reactive SGS scalars and toward developing improved mixing models, the present work investigates the mixing of the SGS mixture fraction, which plays an important role in determining the combustion regimes and local extinction/reignition characteristics. It is also an important model variable in several LES approaches for nonpremixed combustion, such as the laminar flamelet method and conditional moment closure.

The current understanding of conserved scalar SGS mixing is largely based on the Kolmogorov-Obukhov-Corrsin theory, in which the SGS scalar is considered to possess certain self-similar properties. For example, the conditional scalar increment has close-to-Gaussian probability density function (PDF) in the inertial-range; therefore we expect the scalar FDF to also have self-similar properties. However, our recent investigation of SGS mixing in nonreacting jets[4, 5, 6, 7] showed, for the first time, that the SGS scalar has qualitatively different distributions and structures, depending on the *instantaneous* SGS scalar variance. When the SGS variance is small compared to its mean value, the SGS scalar on average has close-to-Gaussian distributions, and the scalar dissipation depends weakly on the SGS scalar, indicating well-mixed SGS scalar fields. The SGS turbulence is in spectral equilibrium, i.e., the production of the SGS variance is equal to or smaller than the SGS dissipation rate. Such SGS mixture fraction distributions are similar to the scalar PDF in a fully developed scalar field. However, when the SGS variance is large compared to its mean value, the SGS scalar on average has bimodal distributions, indicating highly nonpremixed SGS scalar fields. The conditionally filtered scalar dissipation has a bell-shaped dependence on

the scalar. In a nonpremixed flame the bimodal distributions would indicate that the fuel lean and rich regions of the SGS fields are highly segregated, and that there is a sharp interface separating the two regions, across which there is a large scalar value jump, which can be of the order of the integral-scale fluctuations. Such a conditional SGS structure on average resembles that of a counter-flow diffusion flame, which is a model for laminar flamelets[8]. The SGS scalar is in spectral nonequilibrium. The bimodal FDFs are similar to the scalar PDF in the early stages of binary mixing, and are contrary to the general belief based on Kolmogorov's hypothesis that the conditional distributions in the inertial range are self-similar.

The observed correspondences between FDF and conditionally filtered dissipation for small and large SGS variance are also similar to those between the scalar PDF and the conditional dissipation[4, 5]. This is remarkable because while the scalar PDF and the conditional dissipation are related through the scalar PDF equation, there is no analogous equation relating the conditional FDF and the conditionally filtered dissipation. Therefore, the correspondences suggest that the dynamics of the conditional SGS fields are very similar to fully developed and rapidly evolving scalar fields, respectively.

The well-mixed and the highly nonpremixed SGS mixture fraction fields can potentially have strong influences on the flame structure. The former are consistent with Kolmogorov's turbulence cascade picture; therefore, the SGS scalar fluctuations at the dissipation scales (Corrsin scale, $(D^3/\epsilon)^{1/4}$) follow the Obukhov-Corrsin scaling, where D and ϵ are the molecular diffusivity and the energy dissipation rate, respectively. For such SGS fields to support laminar flamelets, the dissipation-scale fluctuations must be larger than the reaction zone width in the mixture fraction space. This condition is similar to that given by Bilger[9].

For the bimodal SGS fields, however, the scalar value jump between the highly nonpremixed SGS regions are generally of the order of the instantaneous SGS rms value, and hence is much larger than the fluctuations predicted by the Obukhov-Corrsin scaling. Furthermore, the jump often occurs over a distance of the order of the Corrsin scale, thereby limiting the reaction zone to

a layer thinner than the Corrsin length scale and resulting in laminar flamelets. This condition for laminar flamelets is similar to that given by Peters[10]. Therefore, the SGS structure under these conditions can significantly affect the flame structure.

In this work we study experimentally the SGS mixing of the mixture fraction in turbulent partially premixed flames and examine the different SGS mixture fraction distributions and structures. We investigate the characteristics of the filtered mass density function (FMDF) of the mixture fraction,

$$F_{\xi L}(\hat{\xi};\mathbf{x},t) = \langle \rho(\mathbf{x},t)\delta(\xi-\hat{\xi};\mathbf{x},t)\rangle_\ell = \int \rho(\mathbf{x}',t)\delta(\xi-\hat{\xi};\mathbf{x}',t)G(\mathbf{x}-\mathbf{x}')d\mathbf{x}', \quad (1)$$

and the conditionally filtered scalar dissipation rate,

$$\langle \chi|\xi\rangle_\ell = \langle D\frac{\partial\xi}{\partial x_j}\frac{\partial\xi}{\partial x_j}|\xi\rangle_\ell, \quad (2)$$

which is the mixing term in the FMDF transport equation, where ξ, ρ, and D are the mixture fraction, the fluid density, and the diffusivity for the mixture fraction, respectively. The subscripts ℓ and L denote conventional and Favre filtered variables, respectively.

2. Experimental data

We use experimental data obtained in piloted turbulent partially premixed methane flames with a 1:3 ratio of CH_4 to air by volume (Sandia flames D and E, see Ref.[11, 12, 13]). The measurements employed combined line-imaging of Raman scattering, Rayleigh scattering, and laser-induced CO fluorescence. Simultaneous measurements of major species (CO_2, O_2, CO, N_2, CH_4, H_2O, and H_2), mixture fraction (obtained from all major species), temperature, and the radial component of scalar dissipation rate were made. The mixture fraction is calculated using a variation of Bilger's definition, which has been modified by excluding the oxygen terms. The length of the imaging line is 6.0 mm with a measurement spacing of 0.2 mm.

Computing the FMDF and the conditionally filtered scalar dissipation from experimental data

requires spatial filtering of scalar fields. In this work, one-dimensional filtering is employed. While in LES the filtering is generally performed in three dimensions, our previous results have shown that the scalar FDF obtained with one-dimensional filters is similar to that obtained with two-dimensional filters[4, 5], which has been shown to be a very good approximation of three-dimensional filtering, with errors of approximately 5% for the rms resolvable- and subgrid-scale variables[14]. For a similar level of bimodality for the FDF, the SGS scalar variance is somewhat larger for one-dimensional filters than for two-dimensional filters. Consequently, one-dimensional filters are expected to yield similar results. The filter sizes Δ employed in this work are 3.0 and 6.0 mm, respectively.

3. Results and discussions

In this section the results of the measured FMDF and the conditionally filtered dissipation are presented. Unlike a PDF and the conditional dissipation, the FMDF and the conditionally filtered dissipation are random variables, and are therefore analyzed here using their conditional averages. We use the Favre filtered mixture fraction,

$$\langle \xi \rangle_L = \langle \rho \xi \rangle_\ell / \langle \rho \rangle_\ell, \tag{3}$$

and the Favre SGS scalar variance,

$$\langle \xi''^2 \rangle_L \equiv \frac{1}{\langle \rho \rangle_\ell} \int F_{\xi L}(\hat{\xi}; \mathbf{x}, t)(\hat{\xi} - \langle \xi \rangle_L)^2 d\hat{\xi} = \langle \rho \xi^2 \rangle_\ell / \langle \rho \rangle_\ell - \langle \xi \rangle_L^2, \tag{4}$$

as conditioning variables.

3.1. The conditional scalar FMDF

The conditional mixture fraction FMDF, $\langle F_{\xi L} | \langle \xi \rangle_L, \langle \xi''^2 \rangle_L \rangle$, for flame D at $x/D = 15$ for several SGS variance values is shown in Fig. 1b. The filter scale is $\Delta = 3.0$ mm and $\langle \xi \rangle_L$ is set to the stoichiometric mixture fraction, $\xi_s (= 0.35)$, to maximize the probability of the SGS field containing reaction zones. For small SGS variance, e.g. $\langle \xi''^2 \rangle_L \approx 0.0004$, the conditional FMDF is unimodal and generally not far from Gaussian. Such a distribution is similar to those obtained in nonreacting

flows and to the scalar PDF in a fully developed turbulent flow, indicating that the SGS mixture fraction is well mixed. Previous results [4, 5] have shown that the SGS scalar under such conditions is in spectral equilibrium, suggesting that the SGS scalar is consistent with Kolmogorov's cascade picture. Therefore, the average SGS scalar fluctuations decreases with the filter scale, suggesting that the burden on the SGS mixing models decreases.

As the SGS variance increases, the FMDF becomes bimodal, with the bimodality stronger for larger SGS variance, indicating that the rich and lean mixtures in the SGS field (i.e., a grid cell) are essentially segregated. Furthermore, there is a sharp interface (diffusion-layer) separating the two regions, across which there is a large scalar value jump (see the discussion on the conditionally filtered scalar dissipation rate below). This SGS scalar structure is essentially a ramp-cliff structure (see Ref.[15]), with the rich and lean mixtures forming the ramps and the diffusion layer as the cliff. The bimodal FMDF is also similar to the scalar FDF for large SGS variance observed in nonreacting flows [4]. Our previous results also showed that the SGS scalar with a large variance is in spectral nonequilibrium, which, along with the presence of the ramp-cliff structure, suggests that the bimodal SGS scalar is not well described by Kolmogorov's turbulence cascade picture. Because the ramp-cliff structure exists in the subgrid scales for all filter sizes significantly larger than the Corrsin scale as in the context of LES, the burden on mixing models to capture the bimodal FMDF does not decrease with the filter scale.

The value of the Favre filtered mixture fraction has different effects on the unimodal and bimodal conditional FMDFs. For a unimodal FMDF, the shape remains approximately unchanged when $\langle\xi\rangle_L$ increases from 0.35 to 0.45 (Fig. 2a), but the position of the peak shifts rightward to approximately 0.42 (leftward to 0.22 for $\langle\xi\rangle_L = 0.25$, not shown). The close-to-Gaussian distributions indicate that the conditional SGS mixture fraction fields are still well-mixed and diffuse toward $\langle\xi\rangle_L$. For $\langle\xi\rangle_L$ values sufficiently away from ξ_s, the SGS field might not contain any reaction zones. Therefore, the FMDFs of such fields are of less interest and not shown. For a bimodal FMDF, the positions of the two peaks move much less than that of a unimodal FMDF as $\langle\xi\rangle_L$ increases from 0.35 to 0.45, but with the left and right peak values decreasing and increasing respectively,

reflecting the increase in the $\langle\xi\rangle_L$ value. This result indicates that variations of the $\langle\xi\rangle_L$ value only alter the fraction of the fuel-lean region relative to that of the fuel-rich region in the conditionally sampled SGS field.

The conditional FMDFs at different downstream locations (Fig. 1) exhibit similar characteristics to that at $x/D = 15$, being close to Gaussian for small SGS variance and bimodal for large SGS variance. The maximum value of the conditional SGS mixture fraction decreases somewhat with increasing downstream distance. Far downstream the maximum will be significantly less than unity (no pure fuel left). However, the qualitative characteristics of close-to-Gaussian and bimodal distributions are expected to remain the same, as observed in non-reacting jets[4, 16].

The filter scale is an important parameter in LES and it is important to understand how the FMDF varies with it. The results for filter scales of 3.0 and 6.0 mm at $x/D = 15$ (Figs. 1b & 2b) are very similar, further demonstrating that the bimodal FMDF is an inherent property of the SGS scalar with large SGS variance and that the burden on the mixing model to predict the bimodal distributions does not decrease with the filter scale. The results also show that the transition from unimodal to bimodal FMDF for the two filter scales (defined as the point at which the top of the FMDF becomes flat) occurs at approximately $\langle\xi''^2\rangle_L = 0.001$ and 0.002, respectively. The difference is related to the mean SGS variance for $\Delta = 3.0$ mm (0.0025) being smaller than that for $\Delta = 6.0$ mm (0.0034). Previous results[4, 16] have shown that in the fully developed region of a non-reacting jet the scalar FDF essentially can be collapsed by the normalized SGS variance, $\langle\xi''^2\rangle_L/\langle\xi''^2\rangle$, regardless of the filter size (as long as it is sufficiently large compared to the Corrsin scale). The results in Figs. 1b & 2b are qualitatively consistent with the previous results. However, in a developing flow this might not be true. Comparing Figs. 1a & 1b we find that in both cases the transition to bimodal FMDF occurs approximately at $\langle\xi''^2\rangle_L$ =0.001, although the mean values of the SGS variance differ by nearly a factor of 2 (0.0065 vs 0.0034). This result might be because the turbulence is evolving rapidly near the nozzle.

The FMDF results show that the statistical structure of the SGS mixture fraction is qualitatively

different for small and large SGS variance values. For a bimodal FMDF, the difference between the ξ values for its peaks is often larger than the near-equilibrium (or mildly strained flamelets) reaction zone width in the ξ space for the methane flames studied in this work ($\Delta\xi_R \approx 0.23$ [17]). Therefore, such a mixture fraction structure is likely to limit the reaction zones in thin diffusion layers, thereby resulting in laminar flamelets. By contrast, for the well-mixed SGS mixture fraction field for small SGS variance, the turbulence cascade is likely to dominate and the dissipation-scale scalar fluctuations largely follow the Kolmogorov-Obukhov-Corrsin predictions. Therefore, such a SGS scalar is likely to result in distributed reaction zones.

3.2. The conditionally filtered scalar dissipation

The conditionally filtered scalar dissipation, $\langle\langle\chi|\xi\rangle_\ell|\langle\xi\rangle_L, \langle\xi''^2\rangle_L\rangle$, for the same conditions as Fig. 1 is shown in Fig. 3. Similar to the FMDF, $\langle\chi|\xi\rangle_\ell$ also has qualitatively different functional forms for small and large SGS variance. For small $\langle\xi''^2\rangle_L$ it shows a weak dependence on ξ, consistent with the conditional FMDF being unimodal and not far from Gaussian. This result provides further evidence that the SGS mixture fraction is well-mixed. For large $\langle\xi''^2\rangle_L$, the conditionally filtered dissipation becomes bell-shaped, with the maximum value increasing with the SGS variance value. Furthermore, the maximum value occurs at the ξ value where the bimodal FMDF has the minimum, indicating that there is an interface between the highly segregated SGS mixture fraction regions and that the interface is essentially a diffusion layer (cliff) with a thickness of the order of the Corrsin scale. Because the diffusion is toward the center of the diffusion layer (cliff), not $\langle\xi\rangle_L$, mixing models such as the interchange through interaction with the mean (IEM) model can lead to unphysical mixing across the diffusion layer (and the reaction zone).

The FMDF and the conditionally filtered dissipation results suggest that the SGS mixture fraction structure under the condition of large SGS variance is similar to that in the counter-flow model for laminar flamelets. However, Rajagopalan and Tong[16] noted that the lean and rich mixtures in a bimodal SGS scalar generally do not have ξ values of 0 and 1 respectively, a situation similar to that noted by Bish and Dahm[18]. Therefore, the laminar flamelets resulted are not

simple flamelets obtained using $\xi = 0$ and 1 as boundary conditions. The FMDF results show that the boundary conditions for these flamelets are essentially the ξ values for the two FMDF peaks.

The correspondences between the functional forms of the FMDF and the conditionally filtered dissipation are consistent with those observed in nonreacting flows[4, 5], again suggesting that, in spite of the lack of an equation analogous to the scalar PDF equation to relate the conditional FMDF to the conditionally filtered dissipation, the dynamics of the conditional FMDF for small and large SGS variance is very similar to the dynamics of the scalar PDFs in fully developed flows and in the early stages of binary mixing, respectively. The similarities between the above results and those obtained in nonreacting flows also suggest that heat release does not change qualitatively the structure of the SGS mixture fraction fields. However, other aspects of the SGS scalar may still be influenced by heat release.

The conditionally filtered dissipation at $x/D = 15$ for the larger filter scale $\Delta = 6.0$ mm in Fig. 4b. has similar characteristics to those for $\Delta = 3.0$ mm, but the maximum value is much lower for the same large SGS variance value. For example, for $\langle \xi''^2 \rangle_L = 0.052$, the maximum value of $\langle \chi | \xi \rangle_\ell$ is above 400 s^{-1} for $\Delta = 3.0$ mm while it is only near 150 s^{-1} for $\Delta = 6.0$ mm. We argue that this difference is due to two factors. First, the transition from unimodal to bimodal FMDF occurs at a smaller SGS variance value for $\Delta = 3.0$ mm than for 6.0 mm (Figs. 1b and 2b). Consequently, we expect that for a given SGS variance, the bimodality is stronger for the former, and therefore the dissipation is higher. The second factor is the relatively low Reynolds number of the flame. Although the filter sizes employed are not very small compared to the half-width of the mean mixture fraction profile (≈ 7.9 mm[11]), they are already close to the scalar dissipation scales (≈ 0.5 mm in cliffs). Consequently, for the same SGS variance value, the average width of the diffusion layer sampled must be smaller in when the filter size decreases, resulting in a higher in-layer dissipation rate.

The conditionally filtered dissipation for $\langle \xi \rangle_L$ =0.45 (Fig. 4a) has similar functional forms to those for $\langle \xi \rangle_L = 0.35$, in contrast with the larger corresponding changes in the FMDF, especially

for large SGS variance values. Because the peak region of the conditionally filtered dissipation is dominated by the cliff, its weaker dependence on $\langle\xi\rangle_L$ indicates that essentially the same cliff is captured by the conditional sampling procedure. The ramps are sampled differently (see Fig. 2a for FMDF), but they correspond to much lower dissipation values, and therefore do not affect the overall functional form of $\langle\chi|\xi\rangle_\ell$.

Comparisons among the results for the conditionally filtered dissipation at the three downstream locations (Fig. 3) show that the maximum value for $\langle\chi|\xi\rangle_\ell$ at large SGS variance decreases from $x/D = 7.5$ to 15, which is due to two reasons. First, the dissipation length scale generally increases with the downstream distance, resulting in a larger diffusion layer thickness and a smaller $\langle\chi|\xi\rangle_\ell$. The second reason is that for large SGS variance there are extinction events at $x/D = 15$ compared to nearly no extinction at $x/D = 7.5$[19], thereby reducing the scalar diffusivity, and consequently the conditionally filtered dissipation. From $x/D = 15$ to 30 the dissipation length scale further increases, which tends to reduce the $\langle\chi|\xi\rangle_\ell$. However, most extinguished fluid parcels have reignited at this location, which tend to increase $\langle\chi|\xi\rangle_\ell$. Due to these competing effects, the maximum value for the conditional $\langle\chi|\xi\rangle_\ell$ at $x/D = 30$ increases slightly compared to that at $x/D = 15$.

The results for the conditional FMDF (Fig. 2c) and $\langle\chi|\xi\rangle_\ell$ (Fig. 4c) for flame E are similar to those for flame D. The jet velocity is higher in flame E, resulting in higher strain rates and more local extinction events. The higher strain rates tend to result in higher scalar dissipation rates. In addition, local extinction may lead to stronger entrainment since heat release tends to suppress entrainment[20], thereby enhancing the dissipation in cliffs. However, local extinction also tends to reduce the diffusivity and dissipation. Moreover, the higher Reynolds number and possibly the local extinction reduce the local scalar dissipation length scale, potentially resulting in insufficient measurement resolution and lower measured dissipation rate. Probably as a result of these competing effects, the maximum value for $\langle\chi|\xi\rangle_\ell$ for flame E (Fig. 4E) is approximately equal to (or slightly smaller than) that for flame D under the same conditions.

The above results indicate that the SGS mixture fraction fields have different spatial structures

for small and large SGS variance values. We provide in Fig. 5 several examples of conditional SGS mixture fraction and mixture fraction-scalar dissipation profiles. For small SGS variance, the $\chi - \xi$ profiles have no clear structures, consistent with the well-mixed SGS mixture fraction. The rms and dissipation-scale SGS mixture fraction fluctuations are smaller than the reaction zone width $\Delta\xi_R$ (≈ 0.23). The measured scalar dissipation values (even after assuming local isotropy and multiplying them by a factor of three) are smaller than the extinction dissipation rate for a steady laminar flame ($\chi_q = 400\ s^{-1}$ for the fuel considered), indicating that the conditional SGS flame is in the form of quasi-equilibrium distributed reaction zones. For large SGS variance, the SGS ξ profiles show a large jump in mixture fraction (the cliff), effectively limiting the reaction zone to within the structure. The $\chi - \xi$ profiles are also consistent with this structure. Therefore, such SGS fields support laminar flamelets. For several profiles the dissipation (even one component) exceeds the extinction value. Therefore, the local extinction events under such conditions are most likely in the form of flamelet extinction.

The results also suggest that at a given location in a turbulent flame, the SGS reaction zones fluctuate between distributed reaction zones and laminar flamelets because the SGS mixture fraction fields vary from well mixed to highly nonpremixed due to fluctuations in the SGS variance. This cause for the occurrences of both flame structures is different from previous arguments based on the fluctuations in the scalar dissipation rate due to turbulence cascade. The scalar dissipation rate at a point, by itself, does not provide sufficient information about the structure of the local mixture fraction field. The variations of the flame structure with the SGS mixture fraction structure suggest that mixing models need to be able to capture the well-mixed and bimodal distributions to account for these flame structures.

To further understand the impact of the SGS mixture fraction structure on the flame structure, it is important to quantify the potential contributions to the heat release from each type of flame structure. We first quantify the portion of the SGS fields containing ramp-cliff structures by plotting the PDF of $ln\langle\xi''^2\rangle_L$ in flame D at $x/D = 15$ (Fig. 6). The PDFs are approximately log-normally distributed with the peaks located at about $\langle\xi''^2\rangle_L = 0.0067$ and 0.014, respectively. From the

results of the conditional FMDF we see that the conditional FMDF is already bimodal for $\langle \xi''^2 \rangle_L$ values at the peak location of the $ln\langle \xi''^2 \rangle)_L$ PDF, indicating that well over 30% of the SGS scalar field contains the ramp-cliff structure ($\langle \xi''^2 \rangle_L > 0.005$ and 0.01 for $\Delta = 3$ and 6 mm, respectively).

To quantify the potential contributions to the heat release from the distributed reaction zones and the laminar flamelets, we calculate the ratio of the contributions to the scalar dissipation rate from the portion of the ramp-cliff structure where the reaction zone resides ($\xi \in [\xi_s - \frac{\Delta\xi_R}{2}, \xi_s + \frac{\Delta\xi_R}{2}]$) to those from all the reaction zones as ,

$$\frac{\langle \chi | \xi \in [\xi_s - \frac{\Delta\xi_R}{2}, \xi_s + \frac{\Delta\xi_R}{2}], \langle \xi''^2 \rangle_L > V \rangle}{\langle \chi | \xi \in [\xi_s - \frac{\Delta\xi_R}{2}, \xi_s + \frac{\Delta\xi_R}{2}] \rangle} Prob\{\langle \xi''^2 \rangle_L > V | \xi \in [\xi_s - \frac{\Delta\xi_R}{2}, \xi_s + \frac{\Delta\xi_R}{2}]\}, \qquad (5)$$

because heat release is, to the first order approximation, proportional to the scalar dissipation rate. The results for several V values are given in Tab. 1. For both filter scales the scalar dissipation for large SGS variance ($\langle \xi''^2 \rangle_L > 0.005$ and 0.01, respectively) accounts for more than 50% of the total scalar dissipation within the reaction zones, suggesting that a significant amount of the heat release comes from ramp-cliff structure, although the ramp-cliff structure only occupies a small fraction of the spatial volume. These results indicate that bimodal SGS mixture fraction associated with the ramp-cliff structure and the resulting laminar flamelets play important roles in non-premixed/partially premixed flames.

4. Conclusions

We use data obtained in turbulent partially premixed flames (Sandia flames D and E) to study the SGS mixing of mixture fraction. The Favre filtered mixture fraction and the Favre SGS scalar variance are used as conditioning variables for analyzing the scalar filtered mass density function and the conditionally filtered scalar dissipation.

The results show that for small SGS scalar variance, the FMDF is unimodal regardless of the filter scale, the measurement location, and the filtered mixture fraction value. However, the peak position of the FMDF shifts with the filtered mixture fraction. The conditionally filtered scalar dissipation rate depends weakly on the SGS scalar, indicating that the SGS scalar is well mixed

and the turbulence cascade is likely to dominate the SGS mixing process. Therefore, such a SGS mixture fraction is likely to result in distributed reaction zones.

For large SGS variance, however, the FMDF becomes bimodal and the conditionally filtered scalar dissipation is bell-shaped, indicating the existence of a ramp-cliff structure, which is similar to the mixture fraction profile in the counter-flow model for laminar flamelets. The mixture fraction structure captured does not depend on the filtered mixture fraction value. For the measurement locations considered the difference in mixture fraction values for the two FMDF peaks are generally larger than the reaction zone width in the mixture fraction space ($\Delta\xi_R = 0.23$ for the fuel considered), therefore the SGS mixing field under such conditions support flamelets. These findings are similar to our previous results obtained in nonreacting jets, indicating that heat release does not alter the qualitative characteristics of the SGS mixture fraction fields.

These results suggest that at a given location the SGS flame fluctuates between distributed reaction zones and laminar flamelets, but for reasons different from the argument based on scalar dissipation fluctuations resulted from the turbulence cascade. The strong effects of the bimodal SGS scalar on the flame structure indicate that mixing models need to be able to capture its distributions to account for the different flame structures. The results for the approximate contributions to the heat release from unimodal and bimodal SGS fields suggest that a significant amount of heat release comes from the ramp-cliff structure, further highlighting its importance in flames and the need for mixing models to capture the bimodal FMDF.

The results for the FMDF with two filter sizes suggest that or small SGS variance, the burden on the SGS mixing models decreases with the filter scale because the SGS scalar is likely to follow the Kolmogorov's cascade picture. For larger SGS variance, large scalar value jumps exist in the SGS scalar for all filter scales significantly larger than the Corrsin scale, therefore the burden on the mixing model does not decrease with the filter size.

Acknowledgments

The work at Clemson was supported by the Air Force Office of Scientific Research under Grant

F-49620-02-1-0130 (Dr. Julian M. Tishkoff, program manager) and by the National Science Foundation under grant CTS-0093532 (CAREER award). The work at Sandia was supported by the Division of Chemical Sciences, Geosciences, and Biosciences, the Office of Basic Energy Sciences, the U.S. Department of Energy. We thank Professor Stephen B. Pope for reading the draft paper and providing valuable comments.

References

[1] S. B. Pope, in: *Proceedings of the 23rd Symposium (International) on Combustion*, 1990, pp. 591–612.

[2] P. J. Colucci, F. A. Jaberi, P. Givi, S. B. Pope, *Phys. Fluids* 10 (1998) 499–515.

[3] M. Sheikhi, T. Drozda, P. Givi., F. Jaberi, S. Pope, *Proc. Combust. Inst.* 30 (2005) 549–556.

[4] C. Tong, *Phys. Fluids* 13 (2001) 2923–2937.

[5] D. Wang, C. Tong, *Phys. Fluids* 14 (2002) 2170–2185.

[6] D. Wang, C. Tong, S. B. Pope, *Phys. Fluids* 16 (2004) 3599–3613.

[7] D. Wang, C. Tong, *Proc. Combust. Inst.* 30 (2005) 567–574.

[8] N. Peters, *Prog. Eng. Combust. Sci.* 10 (1984) 319–339.

[9] R. W. Bilger, in: *Proceedings of the Twenty-Second Symposium (International) on Combustion*, 1988, pp. 475–488.

[10] N. Peters, *Turbulent Combustion*, Cambridge University press, Cambridge, England, 2000.

[11] R. S. Barlow, A. N. Karpetis, *Flow, Turb. Combust.* 72 (2004) 427–448.

[12] A. N. Karpetis, R. S. Barlow, *Proc. Combust. Inst.* 30 (2005) 665–672.

[13] R. S. Barlow, A. N. Karpetis, *Proc. Combust. Inst.* 30 (2005) 673–680.

[14] C. Tong, J. C. Wyngaard, S. Khanna, J. G. Brasseur, *J. Atmos. Sci.* 55 (1998) 3114–3126.

[15] C. Tong, Z. Warhaft, *Phys. Fluids* 6 (1994) 2165–2176.

[16] A. G. Rajagopalan, C. Tong, *Phys. Fluids* 15 (2003) 227–244.

[17] J. H. Frank, S. A. Kaiser, M. B. Long, *Proc. Combust. Inst.* 29 (2002) 2687–2694.

[18] E. S. Bish, W. J. A. Dahm, *Combust. Flame* 100 (1995) 457–464.

[19] D. Wang, Ph.D. dissertation, Clemson University, Department of Mechanical Engineering (July 2005).

[20] A. N. Karpetis, R. S. Barlow, *Proc. Combust. Inst.* 29 (2002) 1929–1936.

Table 1: Contributions to the scalar dissipation rate from the ramp-cliff structure ($\langle \xi''^2 \rangle_L > V$) within the reaction zone for different V values.

flame	Δ	$V = 0.001$	0.002	0.005	0.011	0.024
D	3.0mm	0.879	0.739	0.527	0.254	0.049
D	6.0mm	0.981	0.934	0.815	0.532	0.189
E	3.0mm	0.851	0.69	0.451	0.182	0.026
E	6.0mm	0.97	0.901	0.731	0.41	0.102

FIGURE CAPTIONS

Fig. 1. Conditional FMDF in flame D for $\Delta = 3.0$ mm and $\langle\xi\rangle_L = 0.35$. (a) $x/D = 7.5$; (b) $x/D = 15$; (c) $x/D = 30$.

Fig. 2. Conditional FMDF at $x/D = 15$. (a) flame D, $\Delta = 3.0$ mm, $\langle\xi\rangle_L = 0.45$; (b) flame D, $\Delta = 6.0$ mm, $\langle\xi\rangle_L = 0.35$; (c) flame E, $\Delta = 3.0$ mm, $\langle\xi\rangle_L = 0.35$.

Fig. 3. Conditionally filtered scalar dissipation, $\langle\langle\chi|\xi\rangle_\ell|\langle\xi\rangle_L, \langle\xi''^2\rangle_L\rangle$, in flame D. Conditions same as in Fig. 1.

Fig. 4. Conditionally filtered scalar dissipation, $\langle\langle\chi|\xi\rangle_\ell|\langle\xi\rangle_L, \langle\xi''^2\rangle_L\rangle$. Conditions same as in Fig. 2.

Fig. 5. Conditional profiles in flame D for $\langle\xi\rangle_L = 0.35$. $x/D = 15$, $\Delta = 3.0$ mm. (a) and (c) $\chi - \xi$; (b) ξ.

Fig. 6. PDF of $ln(\langle\xi''^2\rangle_L)$ in flame D at $x/D = 15$. $\langle\xi\rangle_L = 0.35$.

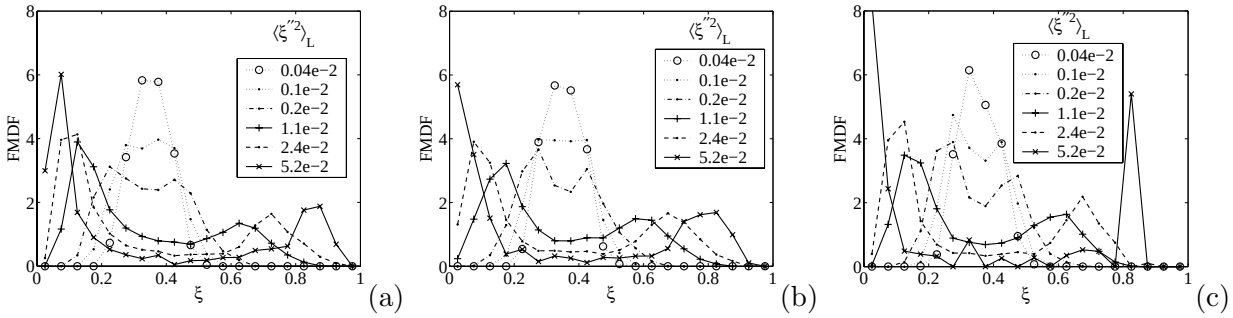

Figure 1: Conditional FMDF in flame D for $\Delta = 3.0$ mm and $\langle\xi\rangle_L = 0.35$. (a) $x/D = 7.5$; (b) $x/D = 15$; (c) $x/D = 30$.

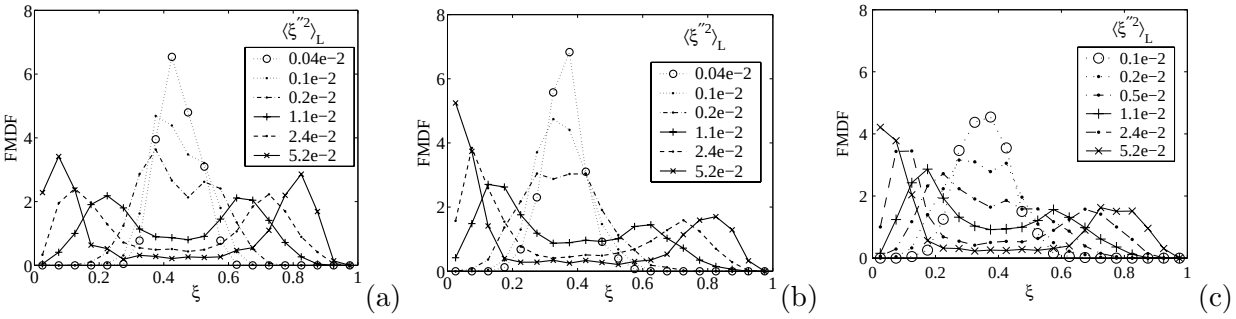

Figure 2: Conditional FMDF at $x/D = 15$. (a) flame D, $\Delta = 3.0$ mm, $\langle\xi\rangle_L = 0.45$; (b) flame D, $\Delta = 6.0$ mm, $\langle\xi\rangle_L = 0.35$; (c) flame E, $\Delta = 3.0$ mm, $\langle\xi\rangle_L = 0.35$.

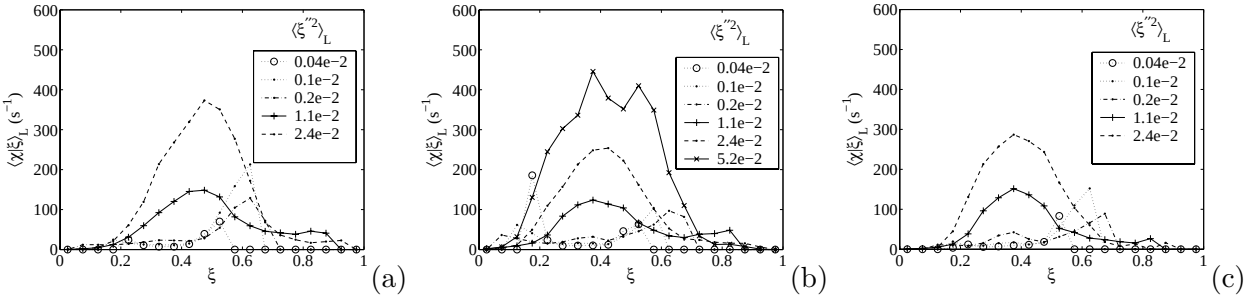

Figure 3: Conditionally filtered scalar dissipation, $\langle\langle\chi|\xi\rangle_\ell|\langle\xi\rangle_L, \langle\xi''^2\rangle_L\rangle$, in flame D. Conditions same as in Fig. 1.

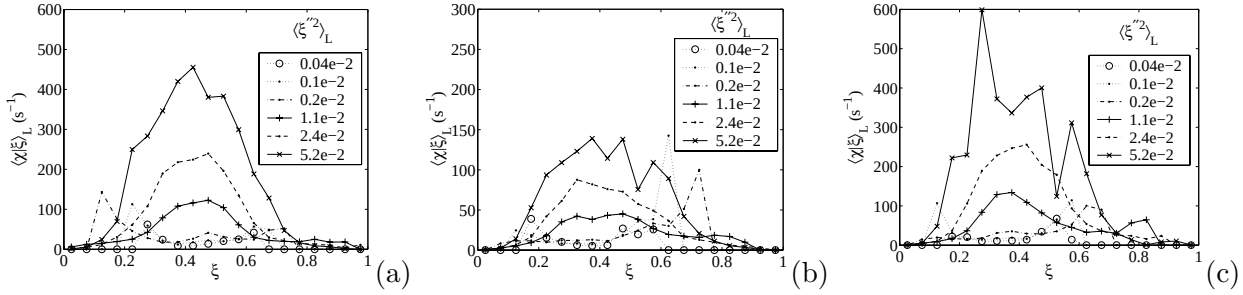

Figure 4: Conditionally filtered scalar dissipation, $\langle\langle\chi|\xi\rangle_\ell|\langle\xi\rangle_L, \langle\xi''^2\rangle_L\rangle$. Conditions same as in Fig. 2.

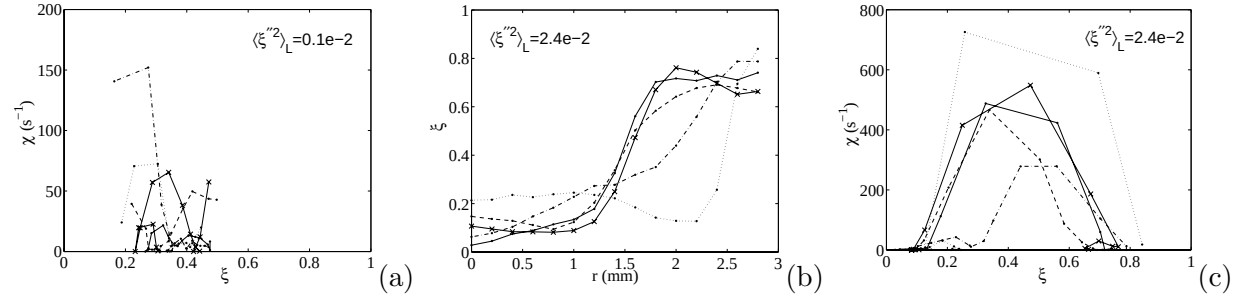

Figure 5: Conditional profiles in flame D for $\langle\xi\rangle_L = 0.35$. $x/D = 15$, $\Delta = 3.0$ mm. (a) and (c) $\chi - \xi$; (b) ξ.

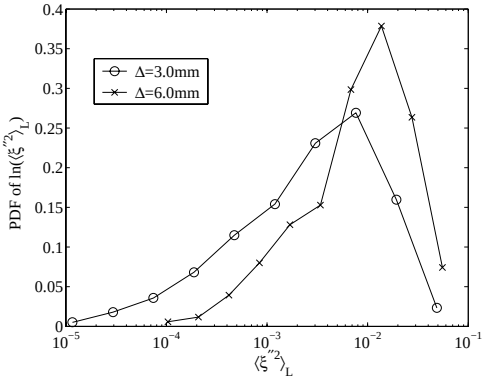

Figure 6: PDF of $ln(\langle\xi''^2\rangle_L)$ in flame D at $x/D = 15$. $\langle\xi\rangle_L = 0.35$.